His-containing plant metallothioneins: comparative study of divalent metal-ion binding by plant MT3 and MT4 isoforms

Mireia Tomas, María Ayelen Pagani, Carlos S. Andreo, Mercè Capdevila, Roger Bofill & Sílvia Atrian

JBIC Journal of Biological Inorganic Chemistry

ISSN 0949-8257
Volume 19
Number 7

J Biol Inorg Chem (2014) 19:1149-1164
DOI 10.1007/s00775-014-1170-1

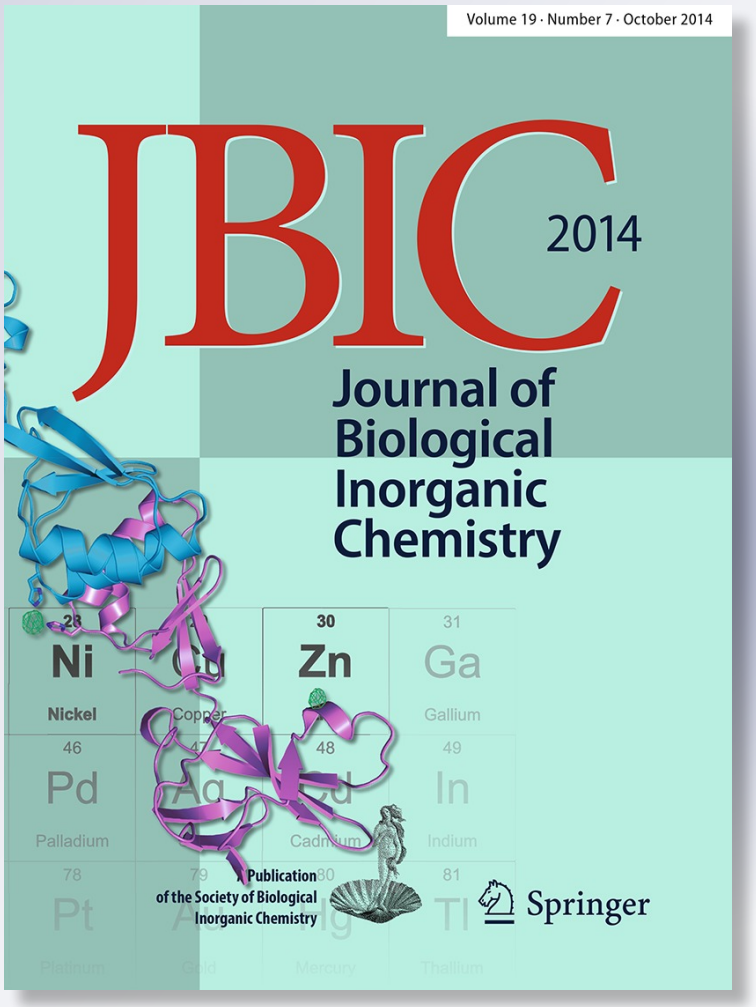

Springer

J Biol Inorg Chem (2014) 19:1149–1164
DOI 10.1007/s00775-014-1170-1

ORIGINAL PAPER

His-containing plant metallothioneins: comparative study of divalent metal-ion binding by plant MT3 and MT4 isoforms

Mireia Tomas · María Ayelen Pagani · Carlos S. Andreo · Mercè Capdevila · Roger Bofill · Sílvia Atrian

Received: 4 February 2014 / Accepted: 31 May 2014 / Published online: 21 June 2014

Abstract Metallothioneins (MTs) are a superfamily of Cys-rich, low-molecular weight metalloproteins that bind heavy metal ions. These cytosolic metallopeptides, which exist in most living organisms, are thought to be involved in metal homeostasis, metal detoxification, and oxidative stress protection. In this work, we characterise the Zn(II)- and Cd(II)-binding abilities of plant type 3 and type 4 MTs identified in soybean and sunflower, both of them being His-containing peptides. The recombinant metal-MT complexes synthesised in Zn(II) or Cd(II)-enriched *Escherichia coli* cultures have been analysed by ESI-MS, and CD, ICP-AES, and UV spectroscopies. His-to-Ala type 3 MT mutants have also been constructed and synthesised for the study of the role of His in divalent metal ion coordination. The results show comparable divalent metal-binding capacities for the MTs of type 3, and suggest, for the first time, the participation of their conserved C-term His residues in metal binding. Interesting features for the Zn(II)-binding abilities of type 4 MTs are also reported, as their variable His content may be considered crucial for their biological performance.

Keywords Plant metallothionein · Zinc · Cadmium · Metal–His binding · Sulphide ligands

Introduction

Metallothioneins (MTs) are small, Cys-rich (ca. 30 % of the amino acid residues) proteins capable of coordinating metal ions such as Zn(II), Cd(II) or Cu(I). Due to the reactivity of the cysteine thiolate groups, MTs show both metal binding and redox activities. Because of these molecular properties [1, 2], several different physiological functions have been proposed for MTs, mainly related to metal homeostasis and detoxification processes, as well as to oxidative stress protection. Being widely spread in nature in all eukaryotes and most prokaryotes, MTs are currently classified into 15 families following taxonomical criteria [3]. Plant MTs, placed in family 15, are further classified into four sub-families based on the patterns of their conserved Cys residues [4]. The p1, p2 and p3 sub-families have two Cys-rich regions, with six Cys at the C-terminal domain and six, eight, and four Cys, respectively, at the N-terminal Cys-rich region; and p4 or pec MTs have three Cys-rich regions containing six, six, and five Cys residues each. Broadly speaking, it could be stated that plant MTs differ from the paradigmatic MT family 1 (mammalian MTs) by exhibiting longer amino acid sequences, even containing some aromatic residues, and a characteristic Cys-free region (or spacer) between their Cys-rich regions (for recent plant MT reviews cf. [5, 6]). These features give rise to the possibility of considering

Electronic supplementary material The online version of this article (doi:10.1007/s00775-014-1170-1) contains supplementary material, which is available to authorized users.

M. Tomas · M. Capdevila · R. Bofill
Departament de Química, Facultat de Ciències, Universitat Autònoma de Barcelona, Cerdanyola del Vallès, 08093 Barcelona, Spain

M. Tomas · S. Atrian (✉)
Departament de Genètica, Facultat de Biologia, Universitat de Barcelona, Av. Diagonal 643, 08028 Barcelona, Spain
e-mail: satrian@ub.edu

M. A. Pagani · C. S. Andreo
Centro de Estudios Fotosintéticos y Bioquímicos, CONICET, Suipacha 531, 2000 Rosario, Argentina

alternative metal-MT complexes where non-cysteine ligands, such as His, could contribute to metal ion coordination. Interestingly, only three 3D structures for His-containing MTs have been solved so far, and with different results regarding His participation in metal binding. Hence, the His residue does not participate in Cu(I)-binding in yeast Cup1 [7] but, contrarily, His is involved in the Zn(II) coordination of wheat Ec-1 [8] and in Zn(II)- or Cd(II)-binding in *Synechococcus* SmtA [9], to build an $M(II)_4(SCys)_9(NHis)_2$ aggregate. Despite the presence of His being rather unusual in most MT families, at least one representative of each sub-family (p1, p2, p3 or pec) of plant MTs contains one or more His residues.

Type 3 plant MTs (p3 sub-family, MT3 from now on) contain ten Cys residues within two Cys-rich domains and they are further subdivided into subtypes, since some of them exhibit additional potential metal ligands, either Cys or His residues, in their sequences [10] (cf. Table S1). Hence, a few MT3 peptides display additional Cys residues, located at their C-term Cys-rich domains, except for *Noccaea caerulescens* MT3. However, and most significantly, either one or two His residues are also present. If there is only one His, it nearly always constitutes the MT3 C-terminus. If there is a second His, it is located in the spacer region, either central or near the second Cys-rich domain. The only exceptions to this general rule are found in the barley MT3 and in the A2Y1D7 rice MT3 isoform. Very little is known about the plant MT3 metal-binding abilities, thus little information is available on the role of the conserved His occurring in their sequences. Hence, the MT3-A-GST fusion protein from palm oil (*Elaeis guineensis*) was reported to bind 1.7 Zn(II) ions more than the GST tag alone when expressed in Zn-enriched *Escherichia coli* cells [11]. On the contrary, banana (*Musa acuminata*) MT3, sharing high sequence similarity to *E. guineensis* MT3, and which also includes an additional His residue at the same position, was found to coordinate 4.3 Cd(II) and 3.0 Zn(II) ions. Significantly, incubation of *M. acuminata* Zn_3-MT3 complexes with an excess of Zn(II) led to the incorporation of a fourth metal ion, and the study of its His-to-Ala and His-to-Cys mutants revealed that His46 was essential to obtain this Zn_4-MT3 species [10]. Recombinant MT3 from *N. caerulescens*, containing 11 Cys residues, yielded Cd_5- and Zn_4-complexes as major species detected through ESI-MS [12]. And finally, only undermetallated Zn- and Cd-loaded recombinant complexes (metal:MT ratio ranging 0.00–0.81) were recovered for the *H. vulgare* MT3 isoform [13].

In another scenario, type 4 MTs (p4 or pec sub-family, MT4 from now on) have been the most studied among all plant MTs, probably due to their peculiar amino acid sequence and the availability of native material [14]. In particular, Zn-Ec-1 from wheat (*Triticum aestivum*), the paradigmatic type 4 MT, has been shown to bind up to 6 Zn(II) ions [15, 16]. Its 3D structure, the only one known for a plant MT, reveals how the three Cys-rich regions are organised into two separate coordinating domains, giving rise to a novel $Zn_2(SCys)_6$ cluster (γ domain) [17], and a Zn_4-β_E domain, which contains the first $Zn(SCys)_2(NHis)_2$ site reported in MTs as well as the typical $Zn_3(SCys)_9$ cluster, also present in mammalian βMT domains [8]. The high affinity that this site shows for Zn(II) over Cd(II) suggests a certain degree of metal specificity [18]. Furthermore, His40, but not His32, seems to be critical for the correct folding, and hence for the biological function of Ec-1, as judged by the foldedness of His-to-Cys mutants [19]. Almost all known flowering plant MT4 peptides include two His residues in their central Cys-rich domains, except for *G. max* MT4, for which we previously reported the presence of only one of them [20], and *Camellia japonica* MT4 (JK711196), which lacks the other highly conserved His residue in this sub-family (cf. Table S2). With plant type 4 MTs landscape being dominated by Ec-1 from wheat, only a few MT4 peptides from other species have been studied. As for MT3, unexpected poorly loaded Zn- and Cd-MT4 complexes were detected for barley (*Hordeum vulgare*) MT4 (2.6-3.3 Zn/MT and 0.0–0.12 Cd/MT [13]). The same situation was observed for *Sesame indicum* MT4, with only 2 Zn/MT [21]. Finally, the metal-binding capacity of the MT4a and MT4b isoforms from *Arabidopsis thaliana* have been recently reported [5], coinciding with the Zn_6- and Cd_6-species previously established for wheat Ec-1.

To understand further the His contribution to metal coordination in different plant MTs, we report here the Zn(II) and Cd(II) binding properties of type 3 and type 4 MTs from soybean (*Glycine max*) and sunflower (*Helianthus annuus*), either for their wild type and for some site-directed-mutant forms (Fig. 1). Wild-type MT3 from soybean (GmMT3) contains two His residues, while sunflower MT3 (HaMT3) has only the C-terminal His. The respective C-terminal His-to-Ala mutants H66AGmMT3 and H67AHaMT3 have been constructed in this study for comparative purposes. Sunflower MT4 (HaMT4), equivalent to Ec-1 in terms of Cys and His patterns, and a soybean MT4 isoform (GmMT4), where the second His is naturally substituted by a Tyr, are also analysed. The corresponding Zn- and Cd-complexes of all these MTs have been recombinantly synthesised in metal-enriched *E. coli* cultures. These complexes, together with DEPC-modified forms have been characterised by means of ICP-AES, CD and UV spectroscopies, as well as ESI-TOF mass spectrometry. All the information gathered in this work on the Zn(II) and Cd(II) binding abilities of role sunflower and soybean MT3 and MT4 is summarised in Table 1. These data will contribute to a better understanding of the

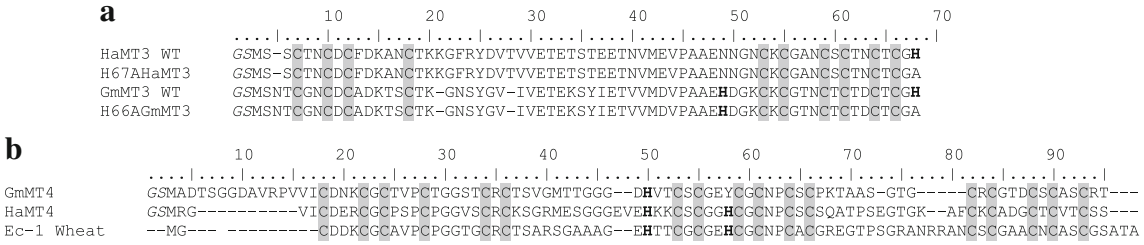

Fig. 1 Amino acid sequences of the peptides studied in this work and of Ec-1 from wheat as reference MT4. Clustal alignment of **a** the type 3 MTs HaMT3 (GenBank accession code DY927914), H67AHaMT3, GmMT3 (CA819971.1) and H66AGmMT3, and of **b** the type 4 MTs GmMT4, HaMT4 (BQ975039) and Ec-1 (SwissProt accession code P30569). The *shaded boxes* indicate the cysteine residues, and histidines are in *bold*. The plasmid derived Gly-Ser dipeptide is shown in *italics*

divalent metal ion coordination features of plant MTs, especially of those encompassing His residues.

Materials and methods

Source of MT cDNA clones

The GmMT3 and GmMT4 clones were previously obtained as reported [20]. The same strategy was followed to obtain the HaMT3 and HaMT4 cDNA clones. To this end, the NCBI basic local alignment search tool (BLAST), namely the nucleotide blastn algorithm, was used to search in the ESTs library database, limiting the results to the *Helianthus annuus* organism. *A. thaliana* metallothionein mRNA sequences NM_112401.1 (MT3) and NM_127888.1 (MT4a) were used as queries. Of the retrieved sequences, those showing a higher number of ESTs, indicative of a higher level of expression for each type of plant MTs, were selected. The ESTs clones DY927914 (HaMT3) and BQ975039 (HaMT4) were acquired from the University of Arizona (The Compositae Genome Project).

Expression vectors construction

Construction of the pGEX-GmMT3 and pGEX-GmMT4 expression plasmids was previously reported [20]. Additionally, the coding region of each of the two sunflower cDNAs, *HaMT3* and *HaMT4*, was subcloned into the pGEX-4T1 plasmid (GE Healthcare). Flanking *BamHI*/*Xho*I restriction sites were added by PCR amplification using the following oligonucleotides: 5′-ATCGGATC CATGTCTTCCTGTACCAAC-3′ as upstream primer and 5′-TATCTCGAGCTAGTGACCACATGTGCA-3′ as downstream primer for *HaMT3*; 5′-ATCGGATCCATGAGGGGT GTTATATGTGACGA-3′ as upstream primer and 5′-TTGCT CGAGTCAAGAGGAACAAGTGACACAAG-3′ as downstream primer for *HaMT4*. For the construction of a cDNA encoding the H66AGmMT3 mutant, the corresponding wild-type sequence was amplified using 5′-GCGGGATC-CATGTCGAACACATGCGGC-3′ as upstream primer, and 5′-AAACTCGAGTTAAGCGCCACAGGTGCA-3′ as downstream primer. The cDNA coding for the H67AHaMT3 peptide was constructed by amplifying the wild-type cDNA using the same upstream primer as for the wild-type cDNA (5′-ATCGGATCCATGTCTTCCTGTACCAAC-3′), but with 5′-TATCTCGAGCTAGGCCCACATGTGCA-3′ as downstream primer.

All PCR reactions consisted of 35-cycle amplifications performed with 1.25 U of GoTaq DNA polymerase (Promega), 0.25 mM dNTPs and 0.20 μM of the required primers at 2 mM $MgCl_2$ (final concentration), in a final volume of 100 μL, under the following cycle conditions: 30 s at 94 °C (denaturation), 30 s at 55 °C (hybridisation) and 30 s at 72 °C (elongation). An initial denaturation step, where samples were heated at 94 °C for 5 min, ensured the complete target DNA denaturation, and elongation conditions were maintained for 7 min after the 35 cycles. The final products were analysed by agarose gel electrophoresis/GelRed Nucleic Acid Gel Stain (Biotium) staining; and the band with the expected size was excised and subcloned into the pGEX-4T1 vector. All the cDNAs were confirmed by automated DNA sequencing. To this end, the pGEX-derived constructs were transformed into *E. coli* MATCH I cells, and plasmids recovered from those cells were sequenced using the ABI PRISM BigDye Terminator v3.1 Cycle Sequencing Kit (Applied Biosystems) in an ABI PRISM 310 Automatic Sequencer (Applied Biosystems).

Recombinant synthesis of MTs

The expression plasmids pGEX-HaMT3, pGEX-HaMT4, pGEX-H67AHaMT3, and pGEX-H66AGmMT3 were individually transformed into the protease defective strain *E. coli* BL21 for the synthesis of the respective GST-MT fusion polypeptides. The recombinant peptides were biosynthesised in 5-L cultures of recombinant *E. coli* BL21 cells. Expression was induced with 100 μM isopropyl β-D-

Table 1 Summary of the Zn- and Cd-binding features of the plant MT3 and MT4 proteins analysed in this work

Zn-MT complex	Zn/MT content[a]	Major Zn-MT species[b]	Major Zn-MT species after Zn(II) addition[b]	CD data[c]	DEPC-modified His[d]	Zn-binding His	His location scheme	Conclusions
HaMT3	3.5	Zn_3, Zn_4	Zn_4	n.i.	0/1	1/0	————————H	C_{term} His binds Zn(II)
H67AHaMT3	2.9	Zn_3	Zn_4	n.i.	0	0	————————	negative control
GmMT3	3.0	Zn_3	Zn_4	n.i.	0/1	2/1	————H——H	central His binds Zn(II)
H66AGmMT3	3.1	Zn_3	Zn_4	n.i.	0	1	————H———	central His binds Zn(II)
HaMT4	6.0	Zn_6	Zn_6	Zn(SCys)	0	2	————H—H—	both His bind Zn(II)
GmMT4	5.6	Zn_5, Zn_6	Zn_6	n.i.	1	0	————H———	His does not bind Zn(II)
Cd-MT complex	**Cd/MT content[a]**	**Major Cd-MT species[b]**	**S^{2-} presence in Cd-complexes**	**CD data[e]**	**DEPC-modified His[d]**	**Cd-binding His**	**His location scheme**	**Conclusions**
HaMT3	4.5	Cd_4	+	His	0	1	————————H	C_{term} His binds Cd(II)
H67AHaMT3	3.1	Cd_4	+/-	---	0	0	————————	negative control
GmMT3	6.2	Cd_4	+	His	1	1	————H——H	C_{term} His binds Cd(II)
H66AGmMT3	4.0	Cd_5S_3,Cd_6S_1	+	---	1	1	————H———	His does not bind Cd(II)
HaMT4	7.7	Cd_6	+	n.i.	2	0	————H—H—	None of the His bind Cd(II)
GmMT4	7.5	Cd_6	+	n.i.	1	0	————H———	His does not bind Cd(II)

[a] Metal per MT molar ratio calculated from the metal and sulphur content measured by acid ICP-AES

[b] Major M(II)-MT species present in the preparations calculated from the difference between holo- and apoprotein molecular masses obtained from ESI-MS

[c] Zn(SCys) means that the typical fingerprint attributed to this chromophore is clearly detected; n.i. stands for non-informative data

[d] This figure corresponds to the number of DEPC-modified residues minus 1, assuming that the N-term peptide residue is always modified

[e] Evidence coming from the analysis of the CD spectra on recombinant preparations and acidified samples; n.i. stands for non-informative data. 'His' means that the effect of His binding to Cd(II) has been observed

thiogalactopyranoside (IPTG) and cultures were supplemented with final concentrations of 300 μM $ZnCl_2$ or $CdCl_2$, and were allowed to grow for a further 3 h. Total protein extract was prepared from these cells, as previously described [22]. Metal complexes were recovered from GST-fusion constructs by batch-affinity chromatography using Glutathione–Sepharose 4B (GE Healthcare) and thrombin cleavage. After concentration using Centriprep Microcon 3 (Amicon), the metal complexes were finally separated from thrombin through FPLC gel filtration in a Superdex75 column (GE Healthcare) equilibrated with 50 mM Tris–HCl, pH 7.0. Selected fractions were confirmed by 15 % SDS-PAGE and kept at −80 °C until use. All procedures were performed using Ar (pure grade 5.6) saturated buffers. Further details on the purification procedure specific for recombinant plant MTs can be found in other related works [23, 24]. As a consequence of the cloning procedure, the dipeptide Gly-Ser is added to the N-terminus of the corresponding MT polypeptides. This minor modification of the native form was previously shown not to alter any of the MT metal-binding capacities [25].

Characterisation of the recombinant metal-MT complexes

The S, Zn and Cd content of all M(II)-MT preparations was analysed by means of inductively coupled plasma atomic emission spectroscopy (ICP-AES) in a Polyscan 61E (Thermo Jarrell Ash) spectrometer, measuring S at 182.040 nm, Zn at 213.856 nm and Cd at 228.802 nm. Samples were treated as previously reported [26], but were alternatively incubated in 1 M HNO_3 at 65 °C for 10 min prior to measurements, in order to eliminate possible traces of acid-labile sulphide ions, as otherwise described [27]. Protein concentrations were calculated from the acid ICP-AES sulphur measurement, assuming that all S atoms were contributed by the MT peptide.

A Jasco spectropolarimeter (Model J-715) interfaced to a computer (J700 software) was used for CD recording at a constant temperature of 25 °C maintained by a Peltier PTC-351S apparatus. Electronic absorption measurements were performed on an HP-8453 diode array UV–visible spectrophotometer. All spectra were recorded with 1 cm capped quartz cuvettes, corrected for the dilution effects and processed using the GRAMS 32 Software.

Molecular mass determinations were performed by electrospray ionisation time-of-flight mass spectrometry (ESI-TOF MS) on a Micro Q-TOF instrument (Bruker) interfaced with a Series 1100 HPLC Agilent pump, equipped with an autosampler, all of them controlled by the Compass Software. Calibration was attained with ESI-L Low Concentration Tuning Mix (Agilent Technologies). Samples containing MT complexes were analysed under the following conditions: 20 μL of protein solution injected through PEEK (polyether heteroketone) tubing (1.5 m × 0.18 mm i.d.) at 40 μL min^{-1}; capillary counter-electrode voltage 5 kV; desolvation temperature 90–110 °C; dry gas 6 L min^{-1}; spectra collection range 800–2,000 *m/z*. The carrier buffer was a 5:95 mixture of acetonitrile:ammonium acetate/ammonia (15 mM, pH 7.0). For analysis of all apo-MTs, 20 μL of the corresponding Zn-MT samples were injected under the same conditions described above, but using a 5:95 mixture of acetonitrile:formic acid pH 2.4 as liquid carrier, which caused the complete demetallation of the peptides.

In vitro Zn(II) and Cd(II) binding studies

Incubation of the Zn-MT samples with excess Zn(II) was carried out by adding five Zn(II) equivalents ($ZnCl_2$) to 15–20 μM solutions of the recombinantly obtained Zn-MT preparations. The mixtures were incubated overnight on ice in Tris–HCl 50 mM pH 7.0. Subsequently, solutions were allowed to reach room temperature, and CD as well as ESI-TOF MS spectra were recorded at pH 7.0. For the Zn(II) with Cd(II) replacement studies, 15–20 μM preparations of the Zn(II)-MT complexes were titrated with incremental amounts of $CdCl_2$ (1–8 equiv) at pH 7.0. CD and UV spectra were recorded immediately after metal addition, and 10 min later, until stable spectra were obtained. All solutions were saturated with Ar to maintain oxygen-free conditions, and all the spectra were corrected for dilution effects.

Analysis of the histidine residues involved in metal ion coordination

Two strategies were used to ascertain whether the His residues of the analysed polypeptides contributed to divalent metal ion coordination. On the one hand, modification of the Zn(II)- and Cd(II)-loaded peptides with diethyl pyrocarbonate (DEPC) was followed by ESI-MS at pH 7.0 (conditions described above). A fresh DEPC solution in absolute ethanol (DEPC:ethanol 1:100) was allowed to react with a ca. 100 μM solution of the tested metal-MT complex in 50 mM Tris–HCl buffer pH 7.0. ESI-MS spectra were recorded at 5- and 24-min reaction times, and molar excess of DEPC was used to ensure the completeness of the modification. The resulting DEPC:polypeptide ratios used were 7:1 for GmMT3, 5:1 for H66AGmMT3, 5:1 for HaMT3, 7:1 for H67AHaMT3, 7:1 for HaMT4 and 5:1 for GmMT4. Half of the values of these DEPC ratios were also assayed in order to obtain more information on the patterns of modification. On the other hand, 10–20 μM preparations of the Cd(II)-MT complexes were acidified

from pH 7.0 to 2.0 with incremental volumes of diluted HCl solutions, and subsequently re-neutralised to pH 7.0 with diluted NaOH. CD and UV spectra were recorded at each step, and all results were corrected for dilution effects. Oxygen-free conditions were maintained by saturation of all solutions with Ar during the experiments.

Results

Identification of the MT genes in sunflower

The in silico analysis of the whole soybean MT system has been recently reported by our group [20]. As regards the sunflower MT system, seven ESTs assignable to the four plant MT types were identified after an in silico NCBI EST database screening. One MT3-type EST was retrieved, which coded for a protein containing the canonical 4- and 6-Cys domains separated by a spacer region of 35 residues long. A single EST also was identified for the MT4 type, encoding a protein containing 17 Cys and 2 His, and matching the typical distribution pattern for this sub-family. These cDNAs were named *HaMT3* and *HaMT4* and the corresponding proteins, HaMT3 and HaMT4, respectively (cf. Fig. 1). The deduced soybean and sunflower MT3 and MT4 polypeptide sequences showed variability in their His content. Soybean MT3 (GmMT3) featured one His located in the spacer region, near the second Cys-rich domain, and a second His in the C-terminal position; whereas sunflower HaMT3 only contained the C-term His. Thus, these MTs represent some of the alternative Cys/His distribution patterns within the MT3 sub-family (cf. Table S1). As already stated before, HaMT4 showed the two conserved MT4 His residues at the Cys-rich central domain, so that the characteristic Cys and His distribution for the MT4 sub-family appeared untouched. On the other hand, soybean MT4 (GmMT4) showed a His-to-Tyr natural substitution for the second His in type 4 plant MTs (cf. Table S2).

Identity, purity and integrity of the recombinant polypeptides

DNA sequencing confirmed that the pGEX constructs for HaMT3, HaMT4, H67AHaMT3 and H66AGmMT3 synthesis included no artifactual nucleotide substitutions, and that the respective cDNAs were cloned in the correct frame after the GST coding sequence. The DNA constructs for GmMT3 and GmMT4 had been previously validated [20]. Recombinant syntheses yielded MT peptides in which their identity, purity and integrity were confirmed by the ESI-MS spectra of the respective apo-forms, obtained by acidification at pH 2.4 of the corresponding Zn-MT complexes. Hence, in each synthesis, a unique polypeptide of the expected molecular mass (including N-terminal Gly-Ser residues derived from the GST-fusion construct) was detected: 7,114.9 ± 0.2 Da for HaMT3 (calculated average mass 7,115.8 Da), 7,048.9 ± 0.1 Da for H67AHaMT3 (calculated 7,049.8 Da); 6,877.7 ± 0.5 Da for GmMT3 (calculated 6,878.7 Da); 6,811.6 ± 0.5 Da for H66AGmMT3 (calculated 6,812.6 Da); 8,451.5 ± 0.3 Da for GmMT4 (calculated 8,452.5 Da); and 8,265 ± 2 Da for HaMT4 (calculated 8,265 Da) (cf. sequences in Fig. 1).

Zn(II)-binding properties of the recombinant MT3 polypeptides

The recombinant syntheses of the four MT3 isoforms were first performed in Zn(II)-enriched *E. coli* cultures: wild-type MT3 from soybean (GmMT3), containing two His residues, sunflower MT3 (HaMT3), with only one C-term His, and the respective C-terminal His-to-Ala mutants H66AGmMT3 (keeping only the His of the spacer region), and H67AHaMT3 (devoid of His). The recovered Zn-MT3 complexes showed Zn(II)-to-MT3 stoichiometries concordant with their Cys content (ten residues), and comparable to those reported before for the GmMT3 isoform [20] (Table 2). In particular, HaMT3 yielded a mixture of major Zn_3- and Zn_4-HaMT3 species (Fig. 2a, upper panel), which correlated well with the mean ca. 3.5 Zn(II)/MT obtained from ICP-AES results (Table 2). In contrast, for

Table 2 Analytical characterisation of the recombinant HaMT3, H67AHaMT3, GmMT3, H66AGmMT3, HaMT4 and GmMT4 preparations synthesised in Zn(II)-enriched media

Protein	His content	Protein concentration of Zn-MT preparations[a] ($\times 10^{-4}$ M)	Zn/MT content[b]	Zn-MT species[c]
HaMT3	1	2.2/2.1	3.6/3.5	**Zn_3, Zn_4** Zn_2
H67AHaMT3	0	2.2/2.4	3.2/2.9	**Zn_3** Zn_2, Zn_4
GmMT3	2	2.1/2.0	2.9/3.0	**Zn_3** Zn_2, Zn_4
H66AGmMT3	1	0.2/0.2	3.0/3.1	**Zn_3** Zn_2, Zn_4
HaMT4	2	1.7/2.0	6.7/6.0	Zn_6
GmMT4	1	1.1/1.2	5.8/5.6	Zn_5, Zn_6

[a] Protein concentration calculated from the sulphur content in normal/acid ICP-AES measurements, respectively

[b] Metal per MT molar ratio calculated from the zinc and sulphur content measured by normal or acid ICP-AES, respectively

[c] Zn-MT species present in the preparations calculated from the difference between holo- and apoprotein molecular masses obtained from ESI-MS. Major species are shown in bold

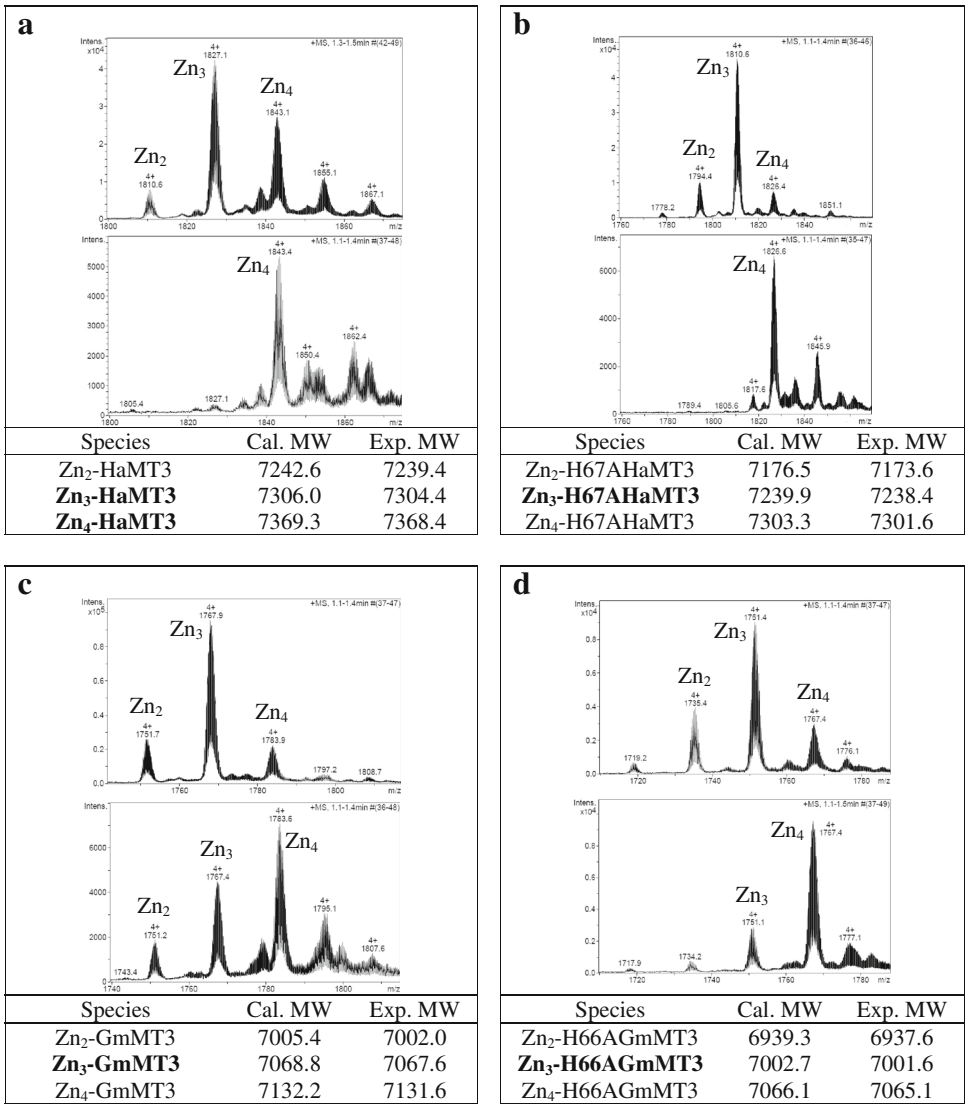

Species	Cal. MW	Exp. MW
Zn_2-HaMT3	7242.6	7239.4
Zn_3-HaMT3	7306.0	7304.4
Zn_4-HaMT3	7369.3	7368.4

Species	Cal. MW	Exp. MW
Zn_2-H67AHaMT3	7176.5	7173.6
Zn_3-H67AHaMT3	7239.9	7238.4
Zn_4-H67AHaMT3	7303.3	7301.6

Species	Cal. MW	Exp. MW
Zn_2-GmMT3	7005.4	7002.0
Zn_3-GmMT3	7068.8	7067.6
Zn_4-GmMT3	7132.2	7131.6

Species	Cal. MW	Exp. MW
Zn_2-H66AGmMT3	6939.3	6937.6
Zn_3-H66AGmMT3	7002.7	7001.6
Zn_4-H66AGmMT3	7066.1	7065.1

Fig. 2 Representative charge states for the ESI-MS spectra recorded at pH 7.0 of recombinant **a** Zn-HaMT3, **b** Zn-H67AHaMT3, **c** Zn-GmMT3 and **d** Zn-H66AGmMT3 before (*above*) and after (*below*) the incubation with an excess of Zn(II) (5 equiv, overnight incubation on ice). The error associated with the experimental MW values was always lower than 0.1 %. Major species in the recombinantly synthesised preparations (*above*) are shown in *bold*

H67AHaMT3, GmMT3 and H66AGmMT3, the major species detected was invariably Zn_3-MT3 (Fig. 2b–d, respectively), in agreement with the approximately 3 Zn(II)/MT measured by ICP-AES in all these cases. Significantly, the comparison between HaMT3 and its mutant form H67AHaMT3 reveals that the His/Ala substitution drastically reduces the presence of the Zn_4-species (Fig. 2a, b, upper panels, respectively), thus strongly suggesting the participation of His67 in Zn(II) binding, at least in the subset of the Zn_4-complexes present in the sample. Contrarily, at this point, no relevant differences are observed between GmMT3 and H66AGmMT3 (Fig. 2c, d, respectively). In order to detect other possible differences in Zn(II) coordination between GmMT3 and HaMT3, all the recovered preparations were Zn-saturated by incubation with an excess of this metal ion [addition of 5 Zn(II) ions per mol of recombinant MT]. Surprisingly, all cases (including H67AHaMT3) rendered the corresponding Zn_4-MT3 complexes as the major species (lower panels in Fig. 2a–d), although clear differences appeared for secondary peaks, which could not be unambiguously attributed. However, it is worth noting that these minor, overmetallated peaks were less important in the His-to-Ala mutants. Unfortunately, the CD spectra of all these preparations exhibited non-informative fingerprints, devoid of clear absorption maxima at the expected wavelengths—i.e. ca. 240 nm—(Fig. 3), which furthermore remained unaltered after exposure to the additional 5 Zn(II) equiv (data not shown). Bearing in mind the canonical Zn_3-$(SCys)_9$ and Zn_4-$(SCys)_{11}$ clusters formed by the mammalian MTs, one could expect that the lack of an 11th ligand would lead to a major Zn_3-species, as is also the case for the *M. acuminata* H46A MT3 mutant [10], bearing 10 Cys, and no His residues. However, this is not the case for H67AHaMT3, as

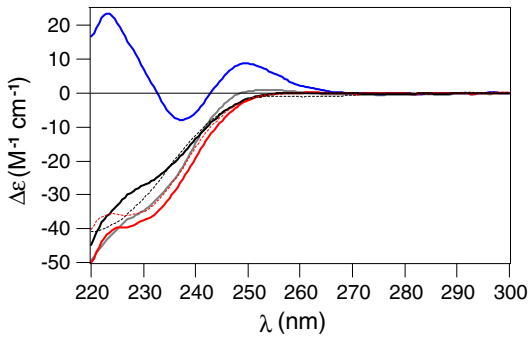

Fig. 3 CD spectra corresponding to recombinant Zn-HaMT3 (*red solid line*), Zn-H67AHaMT3 (*red dashed line*), Zn-GmMT3 (*black solid line*), Zn-H66AGmMT3 (*black dashed line*), Zn-HaMT4 (*blue line*) and Zn-GmMT4 (*grey line*)

our results under excess Zn(II) conditions have clearly demonstrated.

Zn(II)-binding properties of the recombinant MT4 polypeptides

Sunflower MT4 (HaMT4), with a Cys/His pattern identical to Ec-1, and a soybean MT4 (GmMT4), where the second His is naturally substituted by a Tyr, were also synthesised in Zn(II)-supplemented bacterial cultures. A unique Zn_6-HaMT4 species was recovered, while conversely GmMT4 yielded an equimolar mixture of Zn_5- and Zn_6-GmMT4 complexes (Fig. 4a; Table 2), thus reproducing the stoichiometry and speciation reported before [20]. This mixture evolved to an almost unique Zn_6-GmMT4 species only after incubation with a Zn(II) excess (Fig. 4b). The Zn_6-HaMT4 species remained invariable after the addition of an excess of Zn(II) and, exceptionally, when compared to the rest of the Zn-MT preparations analysed here, its CD spectrum (Fig. 3) showed the typical exciton coupling at ca. 245 nm normally associated with the $Zn(SCys)_4$ chromophores [25]. The strict conservation of the His and Cys pattern in Ec-1 and HaMT4 (Fig. 1), and the fact that a unique Zn_6 species was also recovered after recombinant synthesis of Ec-1 in Zn(II)-enriched media [8, 17], strongly supports similar architectures for both Zn(II)-MT4 complexes. Hence, two separate Zn_2-γ and Zn_4-β_E domains, containing a $Zn_2(SCys)_6$ cluster in the former, and both a $Zn(SCys)_2(NHis)_2$ site and a $Zn_3(SCys)_9$ cluster in the latter, could be present in Zn–HaMT4. Furthermore, it has been reported that both the single and double His-to-Ala mutants of Ec-1 rendered a mixture of Zn_5 and Zn_6 species when synthesised in Zn(II)-enriched cultures [19], thus our results for Zn–GmMT4 fit perfectly well within this scenario, since GmMT4 features a H40Y mutation with respect to Ec-1 (numbering refers to Ec-1 sequence; see Fig. 1). Besides, the forced Zn_6–GmMT4 complexes presented the same non-informative CD spectrum as the initial Zn_5– and Zn_6–GmMT4 mixture (data not shown). It is worth noting that recent studies on *A. thaliana* MT4a and MT4b, also encompassing 17 Cys and 2 His residues, coincidently showed the formation of major Zn_6- and Cd_6-species when exposed to Zn(II) or Cd(II), respectively [5]. Therefore, similar metal-binding features are envisaged for all the MT4-type proteins that include 2 His in their sequence (i.e. Ec-1, *A. thaliana* MT4a and MT4b, and HaMT4), in contrast with GmMT4, encompassing a unique His.

Cd(II)-binding properties of the recombinant MT3 and MT4 polypeptides

When HaMT3 or H67AHaMT3 were synthesised in Cd(II)-enriched *E. coli* cultures, a unique Cd_4 species was invariably detected by ESI-MS (Table 3; Fig. 5a, b). Furthermore, the differences observed between the conventional and acid

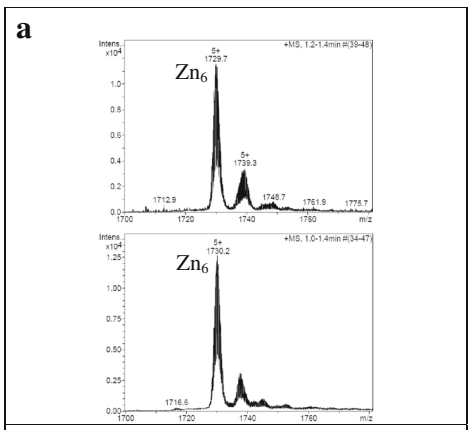

Species	Cal. MW	Exp. MW
Zn_6-HaMT4	8645.7	8645.0

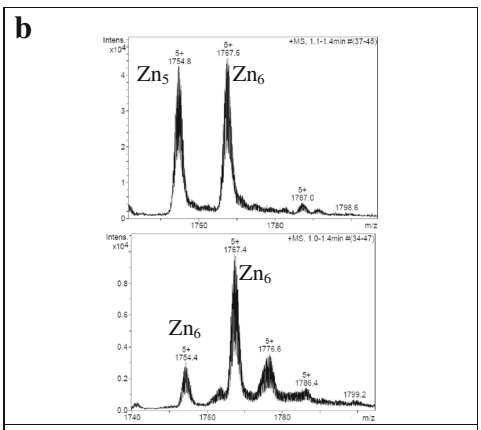

Species	Cal. MW	Exp. MW
Zn_5-GmMT4	8769.4	8769.0
Zn_6-GmMT4	8832.8	8833.0

Fig. 4 Representative charge states for the ESI-MS spectra recorded at pH 7.0 of recombinant **a** Zn-HaMT4 and **b** Zn-GmMT4 before (*above*) and after (*below*) the incubation with an excess of Zn(II) (5 equiv, O.N. incubation on ice). The error associated with the experimental MW values was always lower than 0.1 %

ICP-AES measurements of both preparations (Table 3), as well as their characteristic CD spectra (see below), clearly suggested the presence of some Cd-complexes containing S^{2-} ligands [27], although these species could not be detected by ESI-MS. Cd_4–GmMT3 was also the most abundant species for the *G. max* MT, although here Cd_5 and Cd_6S_1 minor species were also detected (Fig. 5c). Cd-H66AGmMT3 yielded the most heterogeneous sample, including a mixture of species ranging from Cd_4 to Cd_6S_1, with Cd_5S_3 and Cd_6S_1 being the major complexes (Fig. 5d). These results, together with the low amount of protein rendered by the recombinant syntheses, suggested a low stability of the Cd–GmMT3 complexes. The CD spectra of all the Cd-MT3 preparations (Fig. 6a, b) exhibited two types of absorptions: those typical of the $Cd(SCys)_4$ chromophores of the Cd-MT complexes centred at ca. 250 nm [25] and those in the 275–300 nm range, which are related to the presence of S^{2-} ligands as a third component of the Cd-MT species [27]. Although the complex speciation found for both Cd–GmMT3 preparations (ESI-MS spectra; Fig. 5c, d) precluded any assignment of the CD spectra in relation to the participation of the C-term His in Cd(II)-binding (Fig. 6a), the patent difference between the ESI-MS spectra suggested a participation of His66 in Cd(II) coordination. More significant differences were detected when comparing the CD spectra of the Cd_4–HaMT3 and Cd_4–H67AHaMT3 complexes (Fig. 6b). While Cd_4–HaMT3 showed a clear exciton coupling centred at 250 nm, this absorption was far less intense and slightly red-shifted in Cd_4–H67AHaMT3, and the absorption maxima at 280(+) nm of the latter was also red-shifted towards that of the former—at 275 nm. These variations supported the participation of HaMT3 His67 in Cd(II)-binding, despite the apparent similarity of the speciation of both samples shown by ESI-MS (cf. Fig. 5a, b). To further ascertain this point, Cd_4–HaMT3 preparations were

Table 3 Analytical characterisation of the recombinant HaMT3, H67AHaMT3, GmMT3, H66AGmMT3, HaMT4 and GmMT4 preparations synthesised in Cd(II)-enriched media

Protein	His content	Protein concentration of Cd-complexes[a] ($\times 10^{-4}$ M)	Cd/MT content[b]	Cd-MT species[c]
HaMT3	1	1.8/1.1	2.7/4.5	Cd_4
H67AHaMT3	0	1.1/0.8	3.9/3.1	Cd_4
GmMT3	2	0.3/0.3	5.2/6.2	**Cd_4**
				Cd_5, Cd_6S_1
H66AGmMT3	1	0.6/0.5	3.4/4.0	**Cd_5S_3, Cd_6S_1**
				Cd_4, Cd_5, Cd_5S_1
HaMT4	2	1.7/1.5	4.3/7.5	**Cd_6**
				Cd_8S_1
GmMT4	1	1.9/1.3	5.9/7.7	**Cd_6**
				Cd_8S_1

[a] Protein concentration calculated from the sulphur content in normal/acid ICP-AES measurements, respectively

[b] Metal per MT molar ratio calculated from the cadmium and sulphur content measured by normal or acid ICP-AES, respectively

[c] Cd-MT species present in the preparations calculated from the difference between holo- and apoprotein molecular masses obtained from ESI-MS. Major species are shown in bold

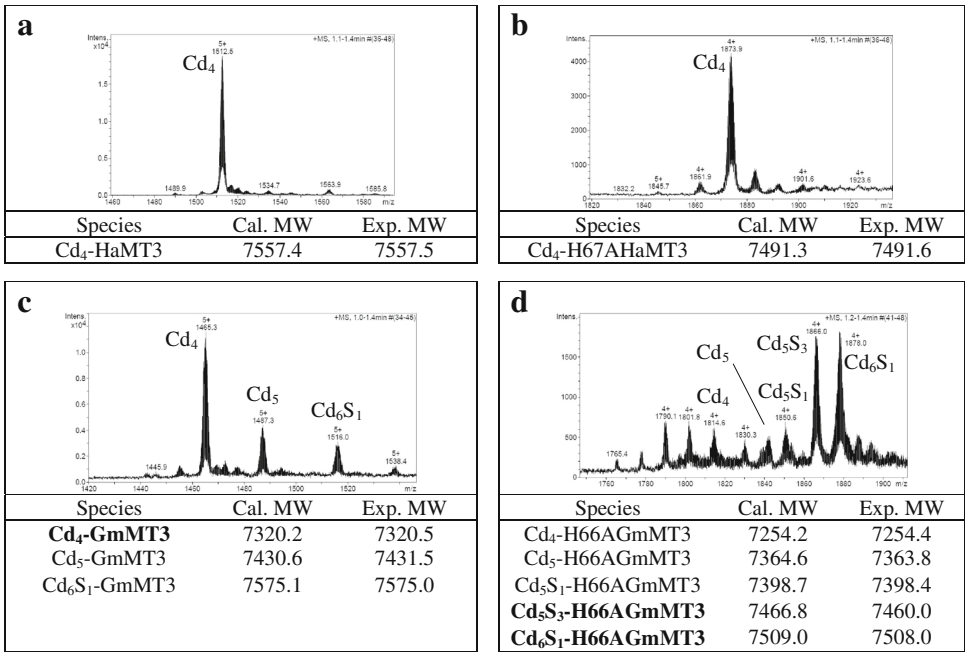

a		
Species	Cal. MW	Exp. MW
Cd_4-HaMT3	7557.4	7557.5

b		
Species	Cal. MW	Exp. MW
Cd_4-H67AHaMT3	7491.3	7491.6

c		
Species	Cal. MW	Exp. MW
Cd_4-GmMT3	7320.2	7320.5
Cd_5-GmMT3	7430.6	7431.5
Cd_6S_1-GmMT3	7575.1	7575.0

d		
Species	Cal. MW	Exp. MW
Cd_4-H66AGmMT3	7254.2	7254.4
Cd_5-H66AGmMT3	7364.6	7363.8
Cd_5S_1-H66AGmMT3	7398.7	7398.4
Cd_5S_3-H66AGmMT3	7466.8	7460.0
Cd_6S_1-H66AGmMT3	7509.0	7508.0

Fig. 5 Representative charge states for the ESI-MS spectra recorded at pH 7.0 of recombinant **a** Cd-HaMT3, **b** Cd-H67AHaMT3, **c** Cd-GmMT3 and **d** Cd-H66AGmMT3. The error associated with the experimental MW values was always lower than 0.1 %. Major species are shown in *bold*

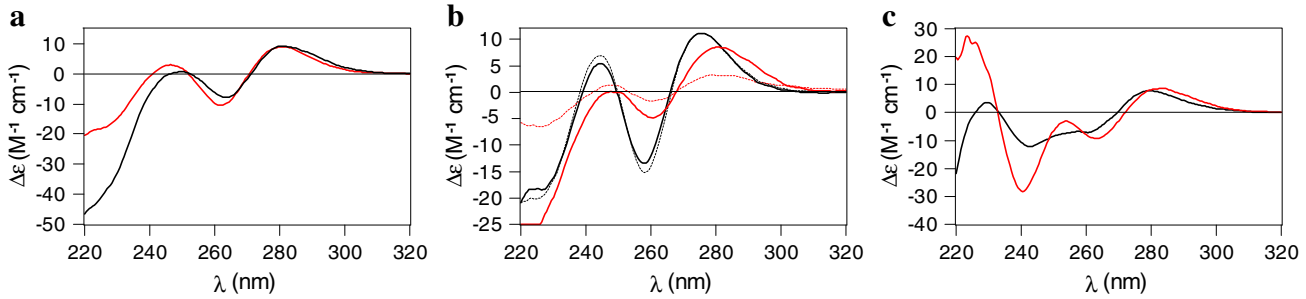

Fig. 6 Comparison of the CD spectra of recombinantly synthesised: **a** Cd-GmMT3 (*black line*) and Cd-H66AGmMT3 (*red line*) at pH 7.0; **b** Cd-HaMT3 at pH 7.0 (*black solid line*), Cd-H67AHaMT3 at pH 7.0 (*red solid line*), Cd-HaMT3 at pH 4.9 (*black dashed line*) and Cd-HaMT3 at pH 4.0 (*red dashed line*); **c** Cd-GmMT4 (*black line*) and Cd-HaMT4 (*red line*)

Fig. 7 Representative charge states for the ESI-MS spectra recorded at pH 7.0 of recombinant **a** Cd-HaMT4 and **b** Cd-GmMT4. The error associated with the experimental MW values was always lower than 0.1 %. Major species are shown in *bold*

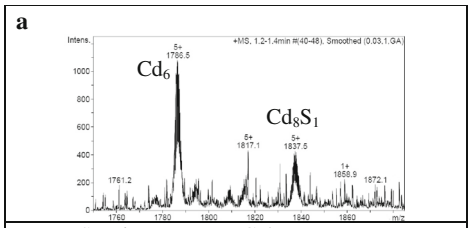

Species	Cal. MW	Exp. MW
Cd_6-HaMT4	8927.8	8927.5
Cd_8S_1-HaMT4	9182.6	9182.3

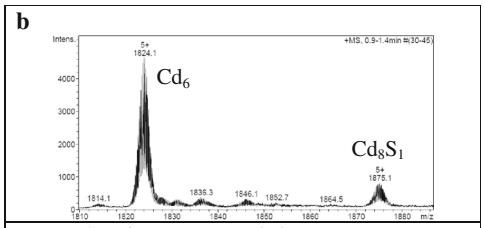

Species	Cal. MW	Exp. MW
Cd_6-GmMT4	9114.9	9115.5
Cd_8S_1-GmMT4	9369.7	9371.0

acidified from pH 7.0 to 2.0, with the rationale that Cd(II) is released from NHis binding sites at a 4–5 pH range owing to His protonation [16], while the lower p*K*a of the cysteine thiolates still allows the existence of CdSCys bonds. Hence, for Cd_4–HaMT3, the initial exciton coupling CD band centred at 250 nm decreased its intensity when lowering the pH from 4.9 to 4.0 (Fig. 6b, Fig. S1), thus generating a CD fingerprint close to that of Cd–H67AHaMT3. In other words, the CD spectra of the preparations of Cd–HaMT3 devoid of His, or when this residue is no longer able to bind Cd(II) because of a solution with a pH lower than the His pKa (i.e. His-to-Ala mutant and Cd-HaMT3 at pH 4.0, respectively), similarly exhibited a poorly resolved exciton coupling band at ca. 255 nm and a positive band at 280 nm. On the other hand, the spectra of Cd–HaMT3 at higher pH, when His is not supposed to be protonated, showed the intense and well-defined exciton coupling band at 250 nm, as well as an intense 275(+) nm band.

With regard to the type 4 MTs, Cd_6 was the major species detected for both GmMT4 and HaMT4, together with a minor Cd_8S_1 form (Fig. 7). Thus, the Cd–GmMT4 recombinant synthesis fully reproduced the previously reported results [20]. Unlike the CD spectra obtained for the Zn(II)-MT complexes, those of the Cd(II) preparations were complex but more informative. Hence, the CD fingerprints of the Cd–HaMT4 and Cd–GmMT4 samples were comparable (Fig. 6c). In this sense, it is interesting to point out that the CD spectrum reported for the recombinantly obtained Cd_6-Ec-1 features a different CD envelope, because it only exhibits a positive Gaussian band centred at 255 nm corresponding to its $Cd(SCys)_4$ chromophores [15]. Contrarily, both Cd-HaMT4 and Cd-GmMT4 CD spectra show comparable absorptions at almost the same wavelengths (although more intense for Cd-HaMT4, and thus compatible with a better folded complex). The clear and coincident absorbance at ca. 280 nm exhibited by both Cd-HaMT4 and Cd-GmMT4 samples are a clear indication of the presence of sulphide ligands in both recombinant preparations [27].

Histidine modification analysis

Diethyl pyrocarbonate is known to covalently modify the free (i.e. non-metal coordinated) histidine residues of proteins with a high efficiency [28–31]. In order to evaluate the number of histidines bound to metal ions in the metal-MT complexes studied in this work, the corresponding Zn- and Cd-MT preparations were incubated with DEPC, and the DEPC-modified derivatives were determined by ESI-MS. As previously reported for other Zn(II)- and Cd(II)-MT complexes, the free terminal α-NH_2 groups also react with DEPC [32], and therefore, when analysing the resulting ESI-MS spectra, at least this carboxyethyl (CEt) species (molecular mass increment of 72.1 Da) should be

detected, and further CEt adducts would reflect the reaction of the non-protected (i.e. metal ion unbound) His residues within the metal-MT complexes present in the preparations. Two times of incubation and two DEPC:protein ratios were tested for each experiment. At the longest time of incubation (24 min), the number and amount of DEPC-modified species detected was comparable for the two doses of DEPC reactant assayed, and thus only the results at the longest time and higher dose conditions are presented here.

Zn-HaMT3 yielded two peaks corresponding to the one- and two-carboxyethylated derivatives (Fig. 8a), while only a mono-carboxyethylated Zn_4 species was identified for the His67Ala mutant (Fig. 8b). Hence, it can be assumed that the two-carboxyethylated Zn_4-HaMT3 species originate from the reaction of His67 with DEPC, thus showing that this residue is unbound for some of the complexes present in the solution. It can be also concluded that two subpopulations of complexes mainly coexist in the Zn-HaMT3 preparation as regards His participation in Zn(II)-binding: one where His67 was DEPC-protected (i.e. involved in metal ion coordination), and another where this His is free. For Zn-GmMT3, two main peaks corresponding to the one- and two-carboxyethylated derivatives were detected, while only a small signal matched the molecular mass of the three-carboxyethylated species (Fig. 8c). Conversely, in the mutant, only one position (presumably its N-terminus) is strongly modified by DEPC (Fig. 8d), and therefore the remaining His (His47) could not be carboxyethylated. These results are in agreement with the existence of one subpopulation of Zn-GmMT3 complexes where both His are involved in Zn(II)-binding, and a subset of complexes where one His is free and the other participates in the metal cluster. Thus, it is suitable to conclude that in GmMT3, His47 would almost always contribute to Zn(II)-binding, while the C-term His66 would only participate in the subset of complexes where both His are coordinating Zn(II). Finally, the three-carboxyethylated species mentioned above would be representative of very minor Zn_4-GmMT3 complexes, where neither His47 nor His66 would be

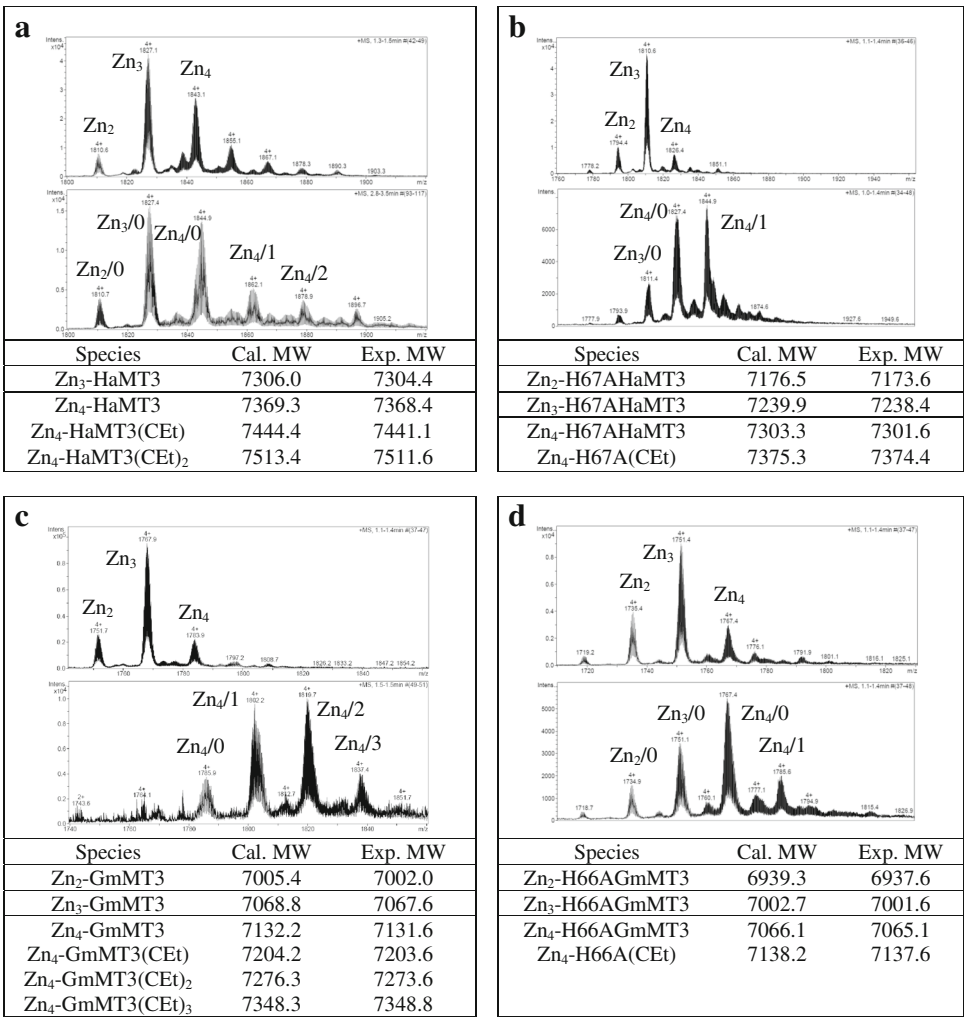

Species	Cal. MW	Exp. MW
Zn_3-HaMT3	7306.0	7304.4
Zn_4-HaMT3	7369.3	7368.4
Zn_4-HaMT3(CEt)	7444.4	7441.1
Zn_4-HaMT3$(CEt)_2$	7513.4	7511.6

Species	Cal. MW	Exp. MW
Zn_2-H67AHaMT3	7176.5	7173.6
Zn_3-H67AHaMT3	7239.9	7238.4
Zn_4-H67AHaMT3	7303.3	7301.6
Zn_4-H67A(CEt)	7375.3	7374.4

Species	Cal. MW	Exp. MW
Zn_2-GmMT3	7005.4	7002.0
Zn_3-GmMT3	7068.8	7067.6
Zn_4-GmMT3	7132.2	7131.6
Zn_4-GmMT3(CEt)	7204.2	7203.6
Zn_4-GmMT3$(CEt)_2$	7276.3	7273.6
Zn_4-GmMT3$(CEt)_3$	7348.3	7348.8

Species	Cal. MW	Exp. MW
Zn_2-H66AGmMT3	6939.3	6937.6
Zn_3-H66AGmMT3	7002.7	7001.6
Zn_4-H66AGmMT3	7066.1	7065.1
Zn_4-H66A(CEt)	7138.2	7137.6

Fig. 8 Representative charge states for the ESI-MS spectra recorded at pH 7.0 for **a** Zn-HaMT3, **b** Zn-H67AHaMT3, **c** Zn-GmMT3 and **d** Zn-H66AGmMT3 before (*above*) and after (*below*) incubation with DEPC. The DEPC-modified peptide includes a carboxyethyl (CEt) group. The numbers in the spectra below indicate the number of CEt groups bound. The error associated with the experimental MW values was always lower than 0.1 %

involved in Zn(II) coordination. Some observations regarding the results of the DEPC treatment are not easy to interpret, but they are in agreement with those observed in a parallel study with the *C. elegans* MT isoforms [32]. They mainly refer to the different DEPC-reactivity exhibited by several complexes of a same MT, or the apparent redistribution of species, even in the absence of DEPC modification. These phenomena could be due to different protein folding, which would condition the availability of reactant to amino acid side-chains, or to a DEPC effect on weak metal-MT bonds, leading to cluster rearrangements.

With respect to Cd-HaMT3, the results on the Cd_4-HaMT3 (Fig. 9a) and Cd_4-H67AHaMT3 (Fig. 9b) complexes mainly indicate a mono-carboxyethylated derivative, which is attributable to the N-term residue modification, and we can therefore conclude that His67 participates in Cd(II)-binding in the wild-type complexes. For Cd-GmMT3, the results were more complex, since a mixture of modified and unmodified species was detected by ESI-MS. For the wild-type protein, one- and two-carboxyethylated derivatives were identified for each one of the initial complexes (Cd_4-, Cd_5- and Cd_6S_1-GmMT3) (Fig. 9c), thus suggesting that one of the GmMT3 His would be always DEPC-protected, while the other would only be protected in a part of the complexes. The three-carboxyethylated species is of less importance than in the corresponding experiment with Zn-GmMT3, so that these data suggest a greater involvement of His in the Cd(II)- than in the Zn(II)-clusters, which can be related to physiological conditions where plant type 3 MTs are induced (discussed below) and/or may be in accordance with the greater bulkiness of Cd(II) ions. Moreover, the presence of two-carboxyethylated Cd_4 and Cd_6S_1 species in the mixture of the DEPC-incubated solution of the Cd-H66AGmMT3 preparation (Fig. 9d) allows us to propose that His66 is most certainly the His residue involved in Cd(II)-

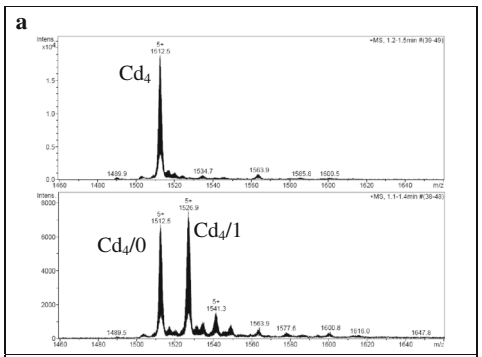

Species	Cal. MW	Exp. MW
Cd_4-HaMT3	7557.4	7557.5
Cd_4-HaMT3(CEt)	7629.5	7629.5

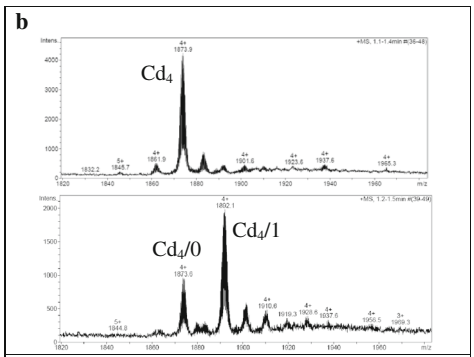

Species	Cal. MW	Exp. MW
Cd_4-H67AHaMT3	7491.3	7491.6
Cd_4-H67A(CEt)	7563.4	7562.4

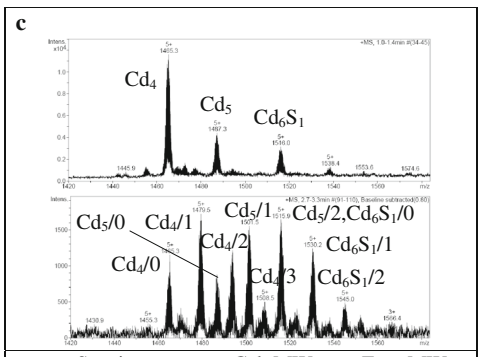

Species	Cal. MW	Exp. MW
Cd_4-GmMT3	7320.2	7320.5
Cd_4-GmMT3(CEt)	7392.3	7392.5
Cd_4-GmMT3(CEt)$_2$	7464.4	7464.5
Cd_4-GmMT3(CEt)$_3$	7536.4	7537.3
Cd_5-GmMT3	7430.6	7431.5
Cd_5-GmMT3(CEt)	7502.7	7502.5
Cd_5-GmMT3(CEt)$_2$	7574.8	7575.0
Cd_6S_1-GmMT3	7575.1	7575.0
Cd_6S_1-Gm3(CEt)	7647.2	7648.0
Cd_6S_1-Gm3(CEt)$_2$	7719.2	7720.0

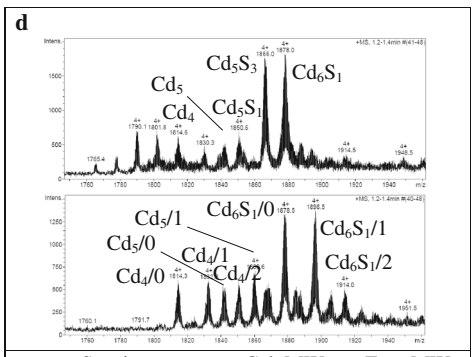

Species	Cal. MW	Exp. MW
Cd_4-H66AGmMT3	7254.2	7254.4
Cd_4-H66A(CEt)	7326.2	7327.2
Cd_4-H66A(CEt)$_2$	7398.3	7398.4
Cd_5-H66AGmMT3	7364.6	7365.2
Cd_5-H66A(CEt)	7436.6	7438.4
Cd_5S_1-H66A	7398.7	7398.4
Cd_5S_3-H66A	7466.8	7460.0
Cd_6S_1-H66A	7509.0	7508.0
Cd_6S_1-H66A(CEt)	7581.1	7581.2
Cd_6S_1-H66A(CEt)$_2$	7653.2	7652.0

Fig. 9 Representative charge states for the ESI-MS spectra recorded at pH 7.0 for: **a** Cd-HaMT3, **b** Cd-H67AHaMT3, **c** Cd-GmMT3 and **d** Cd-H66AGmMT3 before (*above*) and after (*below*) incubation with DEPC. The DEPC-modified peptide includes a carboxyethyl (CEt) group. The numbers in the spectra below indicate the number of CEt groups bound. The error associated with the experimental MW values was always lower than 0.1 %

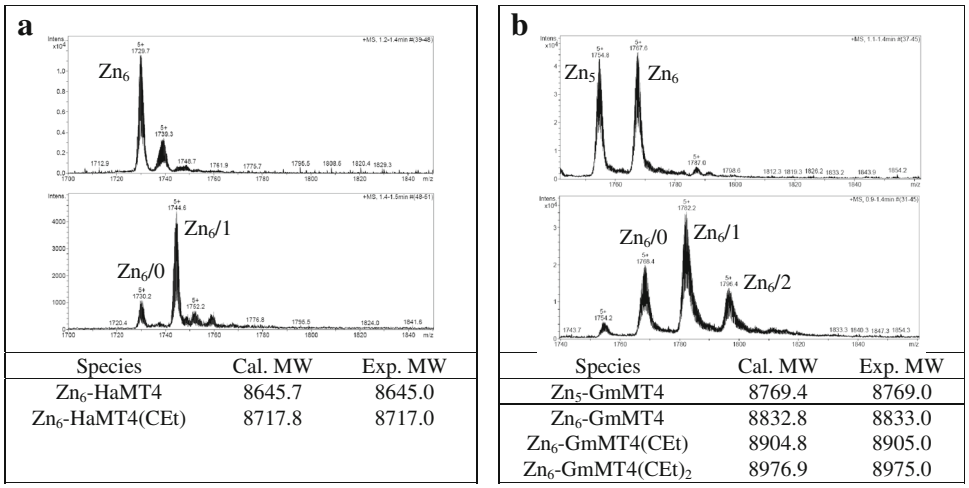

Species	Cal. MW	Exp. MW
Zn_6-HaMT4	8645.7	8645.0
Zn_6-HaMT4(CEt)	8717.8	8717.0

Species	Cal. MW	Exp. MW
Zn_5-GmMT4	8769.4	8769.0
Zn_6-GmMT4	8832.8	8833.0
Zn_6-GmMT4(CEt)	8904.8	8905.0
Zn_6-GmMT4(CEt)$_2$	8976.9	8975.0

Fig. 10 Representative charge states for the ESI-MS spectra recorded at pH 7.0 for: **a** Zn-HaMT4, **b** Zn-GmMT4 before (*above*) and after (*below*) incubation with DEPC. The DEPC-modified peptide includes a carboxyethyl (CEt) group. The numbers in the spectra below indicate the number of CEt groups bound. The error associated with the experimental MW values was always lower than 0.1 %

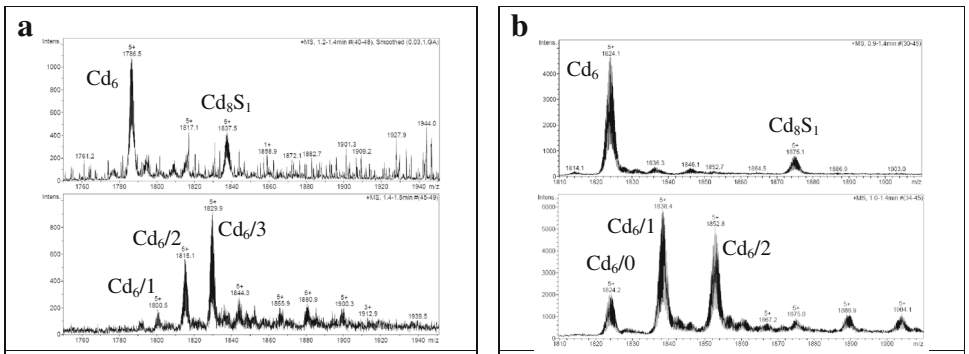

Species	Cal. MW	Exp. MW
Cd_6-HaMT4	8927.8	8927.5
Cd_6-HaMT4(CEt)	8999.8	8997.5
Cd_6-HaMT4(CEt)$_2$	9071.9	9070.5
Cd_6-HaMT4(CEt)$_3$	9144.0	9144.5

Species	Cal. MW	Exp. MW
Cd_6-GmMT4	9114.9	9115.5
Cd_6-GmMT4(CEt)	9186.9	9188.0
Cd_6-GmMT4(CEt)$_2$	9259.0	9258.0

Fig. 11 Representative charge states for the ESI-MS spectra recorded at pH 7.0 for **a** Cd-HaMT4, **b** Cd-GmMT4 before (*above*) and after (*below*) incubation with DEPC. The DEPC-modified peptide includes a carboxyethyl (CEt) group. The numbers in the spectra below indicate the number of CEt groups bound. The error associated with the experimental MW values was always lower than 0.1 %

binding in Cd_4- and Cd_6S_1-GmMT3. This means that the terminal histidine residue is involved in Cd-coordination in both MT3 studied.

The results of the DEPC-reactivity experiments performed with the Zn- and Cd-complexes of the sunflower and soybean MT4 isoforms offered a more straightforward interpretation. Hence, a mono-carboxyethylated derivative is detected for Zn-HaMT4 (Fig. 10a), leading to the conclusion that both His residues contribute to Zn(II)-binding in this complex. Conversely, for Zn-GmMT4, the mono-carboxyethylated derivative is assignable to the product of the reaction with the N-terminal amino group, while the two-carboxyethylated derivative (Fig. 10b) suggests that the unique His present in this polypeptide is mainly not involved in metal ion coordination, since it is accessible to DEPC. Finally, by analogy with the results obtained with Zn-HaMT4 and Zn-GmMT4, it is reasonable to conclude that none of the His residues existing in their sequences are involved in Cd(II) coordination (Fig. 11).

These results enable most of the roles of His residues in divalent metal ion coordination envisaged in the previous sections of this work to be confirmed. Zn-HaMT3 was the exception, where the experiments with DEPC (Fig. 8a) were not completely conclusive, since the amount of DEPC-modified species detected was unexpectedly low. However, the observed differences in stoichiometry for the recombinant wild-type and the His-to-Ala mutant Zn(II)-complexes (Table 2), together with the fact that the Zn/Cd replacement is isostructural for HaMT3 (Fig. S2 and Fig. S3), fully support the previous hypothesis of His67 participating in metal binding in both Zn(II)- and Cd(II)-complexes.

Discussion and conclusions

It can be concluded from the comprehensive interpretation of all the results presented in this work that both soybean

GmMT3 and sunflower HaMT3 feature similar divalent metal ion binding capacities, while substantial differences between soybean GmMT4 and sunflower HaMT4 have been detected. Focusing on His-metal coordination, it should be noted in advance that its occurrence does not always involve the totality of the complexes present in a preparation, but it rather defines a subset of His-contributed Zn- or Cd-species. Two clear examples of His coordination seem to arise from our data: the participation in Zn-binding of both His residues in HaMT4, and the involvement of C_{term} His in the coordination of Cd(II) in both MT3 isoforms studied. It is also patently evident that His would not contribute to Cd-binding in soybean and sunflower MT4. The comprehensive Table 1 summarises the most significant results contributed by this work and the main experimental data that support them.

Regarding the type 3 MTs studied in this work, the results show that both GmMT3 and HaMT3 render major Zn_3- and Cd_4-complexes. GmMT3 encompasses two His residues, in positions 47 and 66, the latter being its C-terminus. Our results suggest that GmMT3 His47 is almost invariably involved in Zn(II)-binding, as it has also been hypothesised for the homologous His in the banana MT3 isoform [10], in which the amino acid sequence is comparable to that of GmMT3 in terms of His47 presence (numbering referring to the GmMT3 protein) and Cys distribution. Otherwise, His66 seems to participate in Zn(II)-coordination, although not in all the Zn(II)-GmMT3 complexes, so that this would establish an equilibrium of species in the preparation. On the other hand, GmMT3 His66, but not His47, seems to participate in Cd(II) coordination, which could be related with the coordinative requirements imposed by the bulkier Cd(II) ions and/or the natural physiological conditions when the peptide performs its function, as discussed below. The former hypothesis is supported by the observation that the minor presence of S^{2-}-containing complexes in the Cd-GmMT3 preparation becomes a major predominance for the corresponding H66A mutant, where sulphide ligands may compensate for the absent His66 additional ligand. In fact, the existence of different subsets of species where an His residue may or may not participate in metal binding has been previously reported for the type 2 MT from cork oak [24], which contains an His within the spacer region that was proposed to participate in Cd(II)-binding in the S^{2-}-devoid preparations, but not in the S^{2-}-containing ones. Regarding HaMT3, the hypothesis of the participation of its unique His67 in both Zn(II)- and Cd(II)-binding is also supported by our results. Again, this C-term His is only involved in a subpopulation of the Zn_4-HaMT3 complexes, while it would be constant for the Cd_4-HaMT3 complexes. In conclusion, our findings point towards a significant involvement of GmMT3 and HaMT3 terminal histidines in Cd(II) coordination. A plausible explanation for this can be related to the natural expression pattern of MT3s and the physiological events in which they are needed. Plant type 3 MT genes are highly expressed in leaves and fruits [5], and many of them, including soybean and sunflower (our unpublished results), are particularly induced during senescence. Leaf senescence is a highly controlled oxidative process that involves degradation of the cellular and sub-cellular structures, and the mobilisation of nutrients from older senescing organs into developing parts of the plant [33]. Breakdown of vacuoles releases both stored mineral nutrients and toxicants, in relation to which it has been hypothesised that plant MTs may play a part in reallocating essential minerals. Here, we propose that type 3 MTs—and not types 1 and 2—may instead have a role in scavenging and immobilising toxic cadmium, preventing its transport to new vegetative tissues or seeds. This function would complement the suggested role of MT3 in the maintenance of Cu homeostasis in plants, as reported in *Thlaspi caerulescens* [34], *Fagopyrum esculentum* [35], *A. thaliana* [36] and *Hordeum vulgare* [13]. C-terminal histidines are highly common among MT3s, and absent in type 1 and 2 plant MTs. Their involvement in Cd-coordination makes the corresponding complexes more resistant to oxidative attack and metal release than a cadmium cluster entirely coordinated by thiolates, since the Cys_3His sites are less nucleophilic and thus less vulnerable to oxidation than the Cys4 ones, as was extensively discussed by Blindauer [37]. Moreover, although it is thought that the ligand variation from Cys to His would increase selectivity towards zinc instead of cadmium according to Pearson's HSAB principle [38], it has to be stressed that the Cys_3His site that must be present in Cd-MT3 complexes would have a similar affinity for either metal ion, in accordance with the dissociation constants determined by Krizec et al. [39]. M(II)-MT3 CD spectra also point towards the preference of these MTs for Cd(II) and the importance of a Cys_3His site since (1) Zn-MT3 spectra exhibited non-informative fingerprints devoid of clear absorption maxima; (2) Cd-MT3 CD spectra showed the typical Cd-MT absorption bands centred at ca. 250 nm; and (3) acidic treatment of Cd-HaMT3 down to a pH below His pKa clearly decreased the overall intensity of the spectrum.

Turning to the Zn(II)-binding abilities of type 4 MTs, HaMT4 binds 6 Zn(II) ions, probably sharing the architecture fully determined for Zn_6-Ec-1 [8, 17] [i.e. a two-domain structure with a $Zn_2(SCys)_6$ cluster at the N-term part and a $Zn_3(SCys)_9$ aggregate plus a single $Zn(SCys)_2(NHis)_2$ site within the C-term moiety]. On the other hand, the presence of a Tyr in position 54 of GmMT4 gives rise to an equimolar mixture of Zn_5 and Zn_6 species, coincident with the results for the replacement of either one or both His in the Ec-1 protein [19]. In contrast,

spectroscopic and spectrometric data led to the conclusion that both GmMT4 and HaMT4 bind 6 Cd(II) ions with no participation of their His residues, as has already been proposed for wheat Cd_6-Ec-1 [5]. Significantly, for both cases, minor Cd_8S_1-MT4 complexes could be clearly detected in the recombinant preparations, this also highlighting their similar Cd(II) coordination abilities. Although the 3D structures of the corresponding metal complexes are needed in order to corroborate these architectures, differential Zn(II)-binding preferences are undoubtedly shown for HaMT4 and GmMT4 as a consequence of the variability in the His content, thus envisaging putative differences for the proposed physiological role of zinc seed source for the development of the future plant [14]. A major metabolic event in the germinating seed is the hydrolysis of reserve proteins to provide the growing seedling with the necessary nutrients before photosynthesis is established, a reason why there is an intense proteolytic activity [40]. It has been shown very recently that proteolytic cleavage is much more efficient than oxidation in promoting zinc deliverance from wheat Ec-1. Moreover, it was proposed that the exact position of the cleavage site can also be determinant [41]. Hence, in GmMT4, the substitution of His54 for Tyr can either add a new protease cleavage site or facilitate proteolysis. Many seed proteases, as for instance C2 from soybean, show little or no preference for specific amino acids forming the peptide bond to be cleaved. Instead, its specificity stems from the three-dimensional structure of the native proteins, where peptide bonds in a very flexible surface loop would be readily accessible to proteolytic attack [42]. The comparison of the Zn-GmMT4 and Zn-HaMT4 CD spectra clearly suggests a less structured Zn-complex for GmMT4, which would be more prone to proteolytic attack, thus enhancing zinc transfer to requiring enzymes. On the other hand, the less structured Zn-GmMT4 complex does not jeopardise the ability of soybean seeds to store zinc, as this plant has another type of MT4 (Glyma18g32760), also highly expressed in seeds, with the classical 17:2 Cys and His content to rely on.

Overall, the results emphasise the importance of His residues in plant MTs, especially among type 3 and type 4 isoforms, where His patterns are considerably conserved. The picture presented here for the MT4 isoforms supports the already described idea of the Cys_2His_2 mononuclear site being critical for their Zn(II)-binding properties [18, 19], which does not preclude the existence of the natural variability of His presence. For the MT3 isoforms, the involvement of their His residues in divalent metal ion binding and the way how it would condition their putative biological properties might be understood in two different ways. On the one hand, we show that the C_{term} His in HaMT3 slightly enhances its Zn(II)-binding capacity, maybe in relation to improved Zn-mediated functions (i.e. Zn homeostasis, redox homeostasis). On the other hand, although also participating in metal ion coordination, neither the His of the linker of Zn-GmMT3 nor the His at the C_{term} of both Cd(II)-MT3 complexes substantially modified their respective metal-binding capacities, so that the hypothesis of conferring an improved resistance towards oxidation should be analysed. Non-Cys residues have been shown to exert a profound effect on the metal-binding properties of MTs, the most clear example being the pulmonate snail MTs [43]. The complete sequential identity of Cys residues and a high degree of conserved positions for other amino acids shared between the strict Cd- and Cu-MT snail isoforms illustrates how the second shell of interactions forced by the side-chains of non-chelating amino acids can impose a completely different metal-specific character onto the coordination chemistry of an MT peptide. A less drastic effect, although significant for its reactivity, is seen when a histidine residue of *H. pomatia* HpCuMT is mutated to alanine [44]. It was shown that the presence of His in this peptide decreases the Cu-binding performance of the isoform, thus probably facilitating the transfer of the metal to biomolecules that require copper. The presence of His residues also has deep consequences on reactivity by providing local order through weak interactions, thus reducing conformational flexibility, as seen in SmtA [45]. We can therefore envisage that His residues of soybean and sunflower MT3 and MT4 may have those and/or other effects on their properties, and therefore more subtle in vitro experiments are needed to shed light on metal preferences and reactivities of these particular proteins, as well as insightful in vivo and/or in planta research to unveil the elusive biological function/s of these and other plant MTs.

Acknowledgments This work was supported by the Spanish *Ministerio de Economía y Competitividad*, Grants BIO2012-39682-C02-01 (to SA) and 02 (to MC), which are co-financed by the European Union through the FEDER program, and from CONICET (Argentina) PIP 2011-2013 0061 (to MAP). Authors from both Barcelona universities are members of the 2009SGR-1457 *Grup de Recerca de la Generalitat de Catalunya*. Cooperation with Argentina was financed by the "*Acción Integrada*" Grant AR2009-0011 (Spain) and ES09/02 (Argentina). We thank the *Centres Científics i Tecnològics (CCiT) de la Universitat de Barcelona* (ICP-AES, DNA sequencing) and the *Servei d'Anàlisi Química (SAQ) de la Universitat Autònoma de Barcelona* (CD, UV–Vis, ESI-MS) for allocating instrument time.

References

1. Capdevila M, Atrian S (2011) J Biol Inorg Chem 16:977–989
2. Capdevila M, Bofill R, Palacios O, Atrian S (2012) Coord Chem Rev 256:46–62
3. http://www.bioc.unizh.ch/mtpage/classif.html. Accessed 5th June 2013
4. Cobbett C, Goldsbrough P (2002) Annu Rev Plant Biol 53:159–182

5. Leszczyszyn OI, Imam HT, Blindauer CA (2013) Metallomics 5:1146–1169
6. Freisinger E (2011) J Biol Inorg Chem 16:1035–1045
7. Calderone V, Dolderer B, Hartmann HJ, Echner H, Luchinat C, Del Bianco C, Mangani S, Weser U (2005) Proc Natl Acad Sci USA 102:51–56
8. Peroza EA, Schmucki R, Güntert P, Freisinger E, Zerbe O (2009) J Mol Biol 387:207–218
9. Blindauer CA, Harrison MD, Parkinson JA, Robinson AK, Cavet JS, Robinson NJ, Sadler PJ (2001) Proc Natl Acad Sci USA 98:9593–9598
10. Freisinger E (2007) Inorg Chim Acta 360:369–380
11. Abdullah SNA, Cheah SC, Murphy DJ (2002) Plant Physiol Biochem 40:255–263
12. Rubio Fernandez L, Vandenbussche G, Roosens N, Govaerts C, Goormaghtigh E, Verbruggen N (2012) Biochim Biophys Acta 1824:1016–1023
13. Hegelund JN, Schiller M, Kichey T, Hansen TH, Pedas P, Husted S, Schjoerring JK (2012) Plant Physiol 159:1125–1137
14. Hanley-Bowdoin L, Lane BG (1983) Eur J Biochem 135:9–15
15. Peroza EA, Freisinger E (2007) J Biol Inorg Chem 12:377–391
16. Leszczyszyn OI, Schmid R, Blindauer CA (2007) Proteins Struct Funct Bioinf 68:922–935
17. Loebus J, Peroza EA, Blüthgen N, Fox T, Meyer-Klaucke W, Zerbe O, Freisinger E (2011) J Biol Inorg Chem 16(5):683–694
18. Blindauer CA (2013) J Inorg Biochem 121:145–155
19. Leszczyszyn OI, White CR, Blindauer CA (2010) Mol Biosyst 6:1592–1603
20. Pagani MA, Tomas M, Carrillo J, Bofill R, Capdevila M, Atrian S, Andreo CS (2012) J Inorg Biochem 117:306–315
21. Chyan CL, Lee TT, Liu CP, Yang YC, Tzen JT, Chou WM (2005) Biosci Biotechnol Biochem 69:2319–2325
22. Capdevila M, Cols N, Romero-Isart N, Gonzàlez-Duarte R, Atrian S, Gonzàlez-Duarte P (1997) Cell Mol Life Sci 53:681–688
23. Domènech J, Mir G, Huguet G, Molinas M, Capdevila M, Atrian S (2006) Biochimie 88:583–593
24. Domènech J, Orihuela R, Mir G, Molinas M, Atrian S, Capdevila M (2007) J Biol Inorg Chem 12:867–882
25. Cols N, Romero-Isart N, Capdevila M, Oliva B, Gonzàlez-Duarte P, Gonzàlez-Duarte R, Atrian S (1997) J Inorg Biochem 68:157–166
26. Bongers J, Walton CD, Richardson DE, Bell JU (1988) Anal Chem 60:2683–2686
27. Capdevila M, Domènech J, Pagani A, Tío L, Villarreal L, Atrian S (2005) Angew Chem Int Ed Engl 44:4618–4622
28. Miles EW (1977) Methods Enzymol 47:431–442
29. Li C, Rosenberg RC (1993) J Inorg Biochem 51:727–735
30. Qin K, Yang Y, Mastrangelo P, Westaway D (2002) J Biol Chem 277:1981–1990
31. Binolfi A, Lamberto GR, Duran R, Quintanar L, Bertoncini CW, Souza JM, Cerveñansky C, Zweckstetter M, Griesinger C, Fernández CO (2008) J Am Chem Soc 130:11801–11812
32. Bofill R, Orihuela R, Romagosa M, Domènech J, Atrian S, Capdevila M (2009) FEBS J 276:7040–7056
33. Prochazkova D, Sairam RK, Srivastava GC, Singh DV (2001) Plant Sci 161:765–771
34. Roosens NH, Bernard C, Leplae R, Verbruggen N (2004) FEBS Lett 577:9–16
35. Nikolić DB, Samardzić JT, Bratić AM, Radin IP, Gavrilović SP, Rausch T, Maksimović VR (2010) J Agric Food Chem 58:3488–3494
36. Guo WJ, Meetam M, Goldsbrough PB (2008) Plant Physiol 146:1697–1706
37. Blindauer CA (2008) J Inorg Biochem 102:507–521
38. Pearson RG (1963) J Am Chem Soc 85:3533–3543
39. Krizek BA, Merkle DL, Berg JM (1993) Inorg Chem 32:937–940
40. Muntz K, Belozersky MA, Dunaevsky YE, Schlereth A, Tiedemann J (2001) J Exp Bot 52:1741–1752
41. Peroza EA, dos Santos Cabral A, Wanz X, Freisinger E (2013) Metallomics 5:1204–1214
42. Seo S, Tan-Wilson A, Wilson KA (2001) Biochim Biophys Acta 1545:192–206
43. Palacios O, Pagani A, Perez-Rafael S, Egg M, Höckner M, Brandstätter A, Capdevila M, Atrian S, Dallinger R (2011) BMC Biol 9:4
44. Perez-Rafael S, Pagani A, Palacios O, Dallinger R, Capdevila M, Atrian S (2013) ZAAC 639:1356–1360
45. Blindauer CA, Razi MT, Campopiano DJ, Sadler PJ (2007) J Biol Inorg Chem 12:393–405